**Photo-responsive hydrogels with photoswitchable mechanical properties allow time-resolved analysis of cellular responses to matrix stiffening**

I-Ning Lee [a,b,1], Oana Dobre [c,d,1], David Richards [d], Christoph Ballestrem [c,d], Judith M. Curran [b], John A. Hunt [e], Stephen M. Richardson [d,*], Joe Swift [c,d,*], Lu Shin Wong [a,*]


[a] Manchester Institute of Biotechnology and School of Chemistry, University of Manchester, 131 Princess Street, Manchester M1 7DN, United Kingdom

[b] School of Engineering, University of Liverpool, Harrison Hughes Building, Liverpool L69 3GH, United Kingdom

[c] Wellcome Trust Centre for Cell-Matrix Research, University of Manchester, Oxford Road, Manchester M13 9PT, United Kingdom

[d] Division of Cell Matrix Biology and Regenerative Medicine, School of Biological Sciences, Faculty of Biology, Medicine and Health, Manchester Academic Health Science Centre, University of Manchester, Manchester M13 9PL, United Kingdom

[e] School of Science and Technology, Nottingham Trent University, Nottingham NG11 8NS, United Kingdom

[1] These authors contributed equally to this work.

* E-mail address: s.richardson@manchester.ac.uk, joe.swift@manchester.ac.uk, l.s.wong@manchester.ac.uk

**Abstract**

As cell function and phenotype can be directed by the mechanical characteristics of the surrounding matrix, hydrogels have become important platforms for cell culture systems, with properties that can be tuned by external stimuli such as UV irradiation, enzymatic treatment and pH. However, many of these stimuli can directly affect cell behaviour, making it difficult to distinguish purely mechanical signalling events. This study reports on the development of a hydrogel that incorporates photoswitchable crosslinkers, which can reversibly alter their stiffness upon irradiation with the appropriate wavelength of light. Furthermore, this study reports the response of bone marrow derived mesenchymal stem cells (MSCs) in these hydrogels that were stiffened systematically by irradiation with blue light. The substrates were shown to be non-cytotoxic, and crucially MSCs are not affected by blue light exposure. Time-resolved analysis of cell morphology showed characteristic cell spreading and increased aspect ratios in response to greater substrate stiffness. This hydrogel provides a platform to study mechano-signalling in cells responding to dynamic changes in stiffness, offering a new way to study mechanotransduction signalling pathways and biological processes with implicit changes to tissue mechanics, such as development, ageing and fibrosis.

**Keywords**

Photoswitchable crosslinkers

Hydrogel

Azobenzene

Mesenchymal stem cells

Morphometrics

Mechanotransduction

## 1. Introduction

Since its inception, *in vitro* cell biology has been performed primarily on rigid substrates, such as glass and polycarbonate, which have Young's moduli ($E$) in the GPa range. This level of rigidity contrasts with most human tissues that are typically more deformable, from "soft" tissues such as marrow ($E \sim 0.2$ kPa)[1] and brain ($E \sim 0.4$ kPa)[2], to "stiff" such as cartilage ($E \sim 24$ kPa)[3] and pre-calcified bone ($E \sim 35$ kPa)[4]. By using synthetic materials fabricated within this range of biological stiffnesses, it is possible to investigate and manipulate cell behaviour in systems that more closely simulate the biomechanics of the tissue microenvironment.[5,6]

Polyacrylamide (PA) based hydrogels have been widely used as a model "soft" material in studies of cell-substrate interaction as they are non-cytotoxic, can be chemically functionalised (e.g. with small molecules, proteins); and have physical properties (e.g. stiffness, porosity) that can be systematically varied by altering their formulation.[7-9] These stiffness-defined substrates have proven to be a valuable tool in efforts to understand cellular mechanotransduction, the transmission of physical inputs into biochemical responses. Indeed, it is now well established that substrate mechanics determines a broad range of cellular behaviours, including cell motility,[10] proliferation[11] and apoptosis[12]. Furthermore mesenchymal stem cells (MSCs), extensively studied because of their potential for application in tissue engineering and regenerative medicine,[13-15] can be mechanically induced to differentiate to lineages commensurate with the substrate stiffness.[4,16] These MSCs are characterised by an ability to adhere to a substrate during *in vitro* culture, and the ability to produce adipogenic, chondrogenic and osteogenic lineages.[17] Biochemically, a diverse range of mechanosensing pathways have been identified, including rapidly responding ion channels;[18] the dynamic interplay between the cytoskeleton, nucleoskeleton and chromatids;[5,16,19,20] the translocation of transcription factors such as YAP1 (yes-associated protein

1)[21], MRTF-A (myocardin-related transcription factor A)[22] and Homeobox protein Nkx-2.5[23]; and mechanically-modulated microRNAs[24].

However, a limitation of current PA-based materials is that their mechanical properties are essentially fixed at the point of preparation. In contrast, developing tissues alter their matrix composition and stiffness in response to mechanical loading.[25,26] For example, fibrosis as a result of a broad range of pathologies is associated with the stiffening of the tissues affected;[27,28] and the ageing process is also known to affect the mechanical properties of many tissues[29]. Thus, studies into the dynamic nature of cell behaviour would greatly benefit from systems that enable a tuneable mechano-environment *in situ*.

To address this aspect, a number of hydrogel systems have been reported that can alter their mechanical stiffness in response to a variety of stimuli while in cell culture. Examples include collagen-alginate formulations that respond to $Ca^{2+}$ ions[30] and pH-sensitive acrylate-based triblock copolymers[31]. However, their use necessitates that the cells are also exposed to these chemical stimuli and it remains unclear if cell behaviour would be unaffected. As an alternative, PA hydrogels that incorporate photocleavable 2-nitrobenzyl-derived crosslinkers have been reported.[32,33] Irradiation with near-UV light (typically ~365 nm) results in the cleavage of these linkers and a softening of the gel, with subsequent changes in cell behaviour. This wavelength of UV irradiation has also been used to activate the crosslinking of methacrylated hyaluronic acid gels, resulting in substrate stiffening.[34] These approaches require only the use of light to trigger the desired mechanical effect, so offer the advantage of being "reagent free". Materials combining different approaches have also been reported. For example, hyaluronic acids bearing both photocleavable crosslinkers and acrylates that are able to repolymerize in the presence of a

photoactivatable polymerization initiator. These materials are able to soften on crosslinker cleavage and stiffen on acrylate polymerization.[35]

Azobenzene is a photo-responsive molecule that undergoes a *trans* to *cis* isomerization upon exposure to UV light (typically between 300-400 nm), resulting in a change of distance between two phenyl rings of ~ 3.5 Å (Figure 1A). Upon irradiation this photoisomerization is rapid and results in a photostationary state (PSS) with ~ 80% of the population in the *cis* state. Conversely irradiation of the *cis* isomers with visible light (typically 400-500 nm) results in a rapid conversion back to the predominantly *trans* form (~ 95% at PSS). Gradual isomerization from *cis* to *trans* forms also occurs thermally.[36,37]
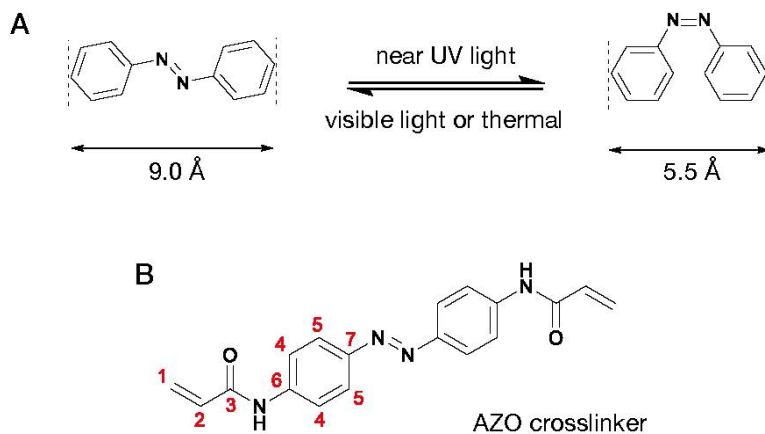


**Figure 1. Structure and isomerization of azobenzene.** (A) Isomerization of azobenzene between *trans* and *cis* isomers. (B) Structure of AZO crosslinker. Numbering in red indicates the positions referred to in the NMR spectra for this compound.

There have been several reports of hydrogels that incorporate an azobenzene group to impart photoswitchable swelling and stiffness changes, for applications in small-molecule (drug)

delivery, cell encapsulation and optical devices.[38,39] There is currently only one example of the use of azobenzene-containing hydrogels in relation to cell culture, in which it is incorporated into a poly(ethylene glycol)-peptide polymer matrix.[40] However, this material has a relatively small dynamic range upon switching (< 1 kPa) and maintains the softer (*cis* isomer) state for a short time (~ 10 h), which limits its usefulness in the context of cell biology.

Building on these examples, this report demonstrates the use of a PA-based hydrogel that incorporates an azobenzene crosslinker for the photoswitchable manipulation of primary human MSCs, demonstrating the potential of this material as a minimally invasive method to study mechanotransduction in this medically important cell type. Here, it is shown that near-UV irradiation results in the softening of the gel while visible blue light results in stiffening, which alters cell morphology.

## 2. Materials and Methods

### 2.1. Materials and equipment

All chemicals were sourced from standard suppliers unless otherwise stated and used without further purification. Antibodies were purchased from Abcam (Cambridge, UK) or Thermo Fisher Scientific (Waltham, MA, USA) and AlexaFluor488-phalloidin from Cell Signalling Technology (Danvers, MA, USA). For cell culture experiments the hydrogels were cast in glass-bottomed dishes (uncoated, γ-irradiated, MatTek Corp, MA, USA).

Irradiation experiments were performed with light emitting diodes (LEDs) emitting at a $\lambda_{max}$ of 365 nm (part no: M365L2) and 490 nm (M490L4), powered by a DC4100 LED driver; all supplied by ThorLabs (Newton, NJ, USA). Photon flux was measured by ferrioxalate actinometry[41,42] with a 3 mL cuvette held 1.3 cm away from the LED, which gave 32.5 and 11.9

mW cm$^{-2}$ for the 365 and 490 nm LEDs, respectively. Epifluorescence microscopy was performed with an Axioplan 2 microscope (Zeiss, Jena, Germany), with the appropriately stained cells (on cover slips) mounted using Fluorescence Mounting Medium (Agilent, Santa Clara, CA, USA). The gold/palladium coater used to prepare samples prior to SEM was a Quorum SC7620 Mini Sputter Coater. SEM images were taken on a XL-30 FEG ESEM (FEI, USA). ESEM images were captured using a Quanta 650 FEG ESEM (FEI).

*2.2. Synthesis of 4,4'-di(acrylamido)azobenzene ("AZO")* [39]

4,4′-azoaniline (265 mg, 1.25mmol) was dissolved in dimethylformamide (DMF, 20 mL) and triethylamine (540 µL, 3.875 mmol) was added, followed by acryloyl chloride (305 µL, 3.75 mmol) in a dropwise manner. The reaction was stirred at room temperature overnight, after which the reaction was observed to be complete by thin-layer chromatography. The solution was poured into 600 mL water and the mixture adjusted to pH 4 by dropwise addition of concentrated aq. HCl. The precipitated orange solids were collected by filtration, washed once each with saturated NaHCO$_3$ and water, then lyophilized to yield the desired product as an orange powder (83.2%, 387.6 mg). $R_f$ 0.38 (EtOAc); $\lambda_{max}$/nm (THF) 377 ($\varepsilon$/dm$^3$ mol$^{-1}$ cm$^{-1}$ 33200); $\nu_{max}$/cm$^{-1}$ (Solid) 3310, 3067, 1670, 1248, 843; $\delta_H$ (400 MHz; DMSO-$d_6$) 5.81 (2H, C(1)H**,** *d, J*=10.1 Hz), 6.31 (2H, C(1)H**,** *d, J*=16.9 Hz) 6.49 (2H, C(2)H, *dd, J*=10.1, 16.9 Hz), 7.88 (8H, C(4,5)H, *m*) and 10.6 (2H, NH, *s*); $\delta_C$ (101 MHz, DMSO-$d_6$) δ 119.41 (C(4)H), 123.56 (C(5)H), 127.74 (C(1)H$_2$), 131.59 (C(2)H), 141.96 (C(6)), 147.82 (C(7)) and 163.48 (C(3)); *m/z* (ES+) 343 (100%, [M+Na]$^+$); HRMS calculated for C$_{18}$H$_{16}$N$_4$O$_2$: 321.1535, found: 321.1352 ([M+H]$^+$), *δ* 2.3 ppm.

*2.3. Fabrication of hydrogels*

The prepolymer mixtures for initial screening were formulated according the compositions specified in the Supporting Information (Tables S1-S6 in SI). In general, AZO was dissolved in dimethylsulfoxide (DMSO), DMF or EtOH. Separately, aqueous solutions of acrylamide (AM, 40% w/v) and *N,N'*-methylenebisacrylamide (BIS, 0.1 M) were mixed with phosphate buffered saline (PBS). The AZO and AM/BIS solutions were then mixed with ammonium persulfate (APS, 10% w/v in water, 10 μL) and *N,N,N',N'*-tetramethylethylenediamine (TEMED, 1 μL). These mixtures were allowed to polymerise in vials for 30 min prior to analysis.

Of the polymer formulations that were subsequently taken for cell culture, mechanical and photochemical characterization (Formulations **56**, **62**, **64** and **83**; see Section 3.1 below), these were cast on glass-bottomed dishes and coated with fibronectin (see Figure S1 in SI for an illustration of the general workflow). The glass surfaces of the dishes were surface treated with aq. NaOH (700 μL, 1M) for 5 min, followed by washing three times with deionized water and drying with a stream of $N_2$ gas. 3-Aminopropyltriethoxysilane (700 μL) was then pipetted onto the glass, left to stand for 5 min and washed three times with water and dried as above. Glutaraldehyde (0.5% v/v in water, 700 μL) was added, incubated for 30 min and the glass was then washed and dried as above.[5] Separately, glass coverslips were prepared by drop coating with a rat fibronectin (FN) solution (120 μL, 0.05 mg mL$^{-1}$ in PBS), which was allowed to stand for 1 hour before drying with a stream of $N_2$ gas. 30 μL of the desired prepolymer mixture was the dropped onto the silanized glass surface of a glass-bottomed dish. The FN-coated coverslip was placed on top of the droplet, taking care to ensure even spreading of the prepolymer droplet and avoidance of any trapped bubbles. The polymerization was allowed to proceed for 30 min, after which the coverslip was carefully removed and the FN-coated hydrogels stored in the dark under PBS at 25 °C until used.

For cell culture, the hydrogels were prepared according to formulation **83** (see SI for composition). For calibration purposes, FN-coated PA gels with defined stiffnesses of 2, 4, 8 and 23 kPa were prepared according to previously published formulations.[9]

*2.4. UV-Vis absorption spectroscopy and photoirradiation*

UV-Vis spectra of the AZO crosslinker in solution were measured at a concentration of 21 µM in tetrahydrofuran in a 1 cm pathlength glass cuvette. For the irradiation of solutions, the same solution was placed in a cuvette holder (ThorLabs CVH100) directly coupled to the desired LED. During irradiation, the samples were removed intermittently and the UV-Vis spectrum recorded, before returning the sample for further irradiation.

The proportions of the isomers at the PSS was calculated using a similar method as previously reported.[43,44] Under 365 nm irradiation (*trans* to *cis*), the following formula was used:

$$f_{365} = \frac{A_E - A_{PSS365}}{A_E - A_Z}$$

Where $f_{365}$ is the fraction of the AZO population that is in the *cis* state at the PSS under 365 nm irradiation; $A_E$ is the absorbance at the $\lambda_{max}$ (in this case 380 nm) of the AZO solution before irradiation, which is assumed to be 100% *trans* isomer; $A_{PSS365}$ is the absorbance at 380 nm at the PSS under 365 nm irradiation (for this calculation, the absorbance after 100 s irradiation was used); $A_Z$ is the theoretical absorbance at 380 nm of the AZO solution at 100% *cis* isomer, which for this calculation was taken to be zero (i.e. absorbance after subtraction of the solvent baseline).

For the spectral measurements at 490 nm (*cis* to *trans*), the AZO solution was irradiated continuously for 30 min with 365 nm light, then irradiated at 490 nm for various time intervals with periodic UV-vis data collection. The $f_{490}$ was calculated using:

$$f_{490} = 1 - \left(\frac{A_E - A_{PSS490}}{A_E - A_Z}\right)$$

Where $f_{490}$ is the fraction of the AZO population that is in the *cis* state at the PSS under 490

nm irradiation; $A_E$ is the absorbance at the $\lambda_{max}$ (in this case 380 nm) of the AZO solution before

irradiation at 365 nm, which is assumed to be 100% *trans* isomer; $A_{PSS490}$ is the absorbance at 380

nm at the PSS under 490 nm irradiation (for this calculation, the value after 100 s irradiation at

490 nm was used); $A_Z$ is the theoretical absorbance at 380 nm of the AZO solution at 100% *cis*

isomer, which for this calculation was taken to be zero (i.e. absorbance after subtraction of the

solvent baseline).

For the irradiation of the hydrogels, the petri dish containing the hydrogel (from Section

2.3) was placed on a Peltier cooler set to 25 °C, and PBS was added sufficient to keep the gel from

drying (approximately 200 µL). The LED was placed 1 cm above the gel. At the appropriate time

intervals, the petri dish was removed, any excess PBS drained, the dish (with the gel in place)

placed in a UV-vis spectrometer and its spectra recorded. The dish and gel were then returned to

the Peltier cooler, PBS added and irradiation restarted until the next time interval, when the process

was repeated.

*2.5. Atomic force microscopy (AFM) of hydrogels*

Hydrogel stiffness was measured by AFM using either: (i) JPK CellHesion AFM using

tipless cantilevers (Bruker NP-O10) attached to 10 µm diameter stiff polystyrene beads (Kisker

Biotech PPS-10.0) using Loctite 3103 UV curing glue. The gels were immersed in PBS during the

measurements. Measurements were made in randomly selected 30 µm x 30 µm areas on each

hydrogel; two measurements were obtained at each point of an array of 4 x 4 in each area. (ii)

Bruker Catalyst AFM coupled with a Nikon Eclipse Ti microscope, operated in peak force tapping

mode using a cantilever tipped with a 5 µm-diameter borosilicate glass sphere (CP-CONT-BSG-A; sQUBE, Windsor Scientific, UK). Hydrogels were immersed in deionized water as measurements were made in randomly selected 10 µm x 10 µm areas. The force constant of the cantilever was measured by thermal tuning in air. Force curve data was fitted using the Hertz model.[45] Comparative experiments between the two instruments using the same samples confirmed that the data was mutually comparable.

## 2.6. Scanning electron microscopy (SEM) and environmental SEM of hydrogels

For SEM, the hydrogels were snap frozen in liquid nitrogen then lyophilized. Prior to imaging, hydrogels were attached to a metallic holder using double-sided tape and sputtered with gold/palladium alloy for 90 s. Images were recorded using an accelerating voltage of 10 kV.

ESEM images of hydrogels were captured in variable pressure mode at 1.3 mBar using water vapour as the make up gas. The instrument was operated at an accelerating voltage of 10 kV and secondary electron images were collected with a large field detector.

## 2.7. Isolation and culture of mesenchymal stem cells (MSCs)

Human MSCs were isolated from the bone marrow (knee and hip) of male and female donors aged 58 – 80 years using a previously reported methodology.[46] The relevant ethical approvals were obtained in all cases prior to the procedures. MSC cultures were expanded on tissue culture treated polystyrene (TCTP) in low-glucose Dulbecco's modified Eagle's medium (DMEM) with pyruvate, 10% fetal bovine serum (FBS) and 1 % penicillin/streptomycin solution (containing 10,000 units of penicillin and 10 mg streptomycin per mL); under an atmosphere of 5.5 % $CO_2$ at

37 °C. Cell interactions with substrates were characterized using cells at passage five or lower. DMEM without phenol red was used in irradiation experiments.

## 2.8. Assessment of cell viability

MSCs were seeded on coverslips at a density of 2 x $10^4$ cells cm$^{-2}$ 24 h prior to irradiation. Cells were exposed to light from the desired LED source for defined periods of time, then cultured for a further 24 h before cell viability was assayed with the LIVE/DEAD Viability/Cytotoxicity kit (ThermoFisher) according to the manufacturer's instructions.

## 2.9. Quantification of DNA damage

MSCs were seeded on coverslips at a density of 2 x $10^4$ cells cm$^{-2}$ 24 h prior to irradiation. Cells were exposed to light from either LED source for the desired period of time, then cultured for a further 24 h before being fixed with 4% formaldehyde in PBS for 10 min, followed by two 5 min washes with PBS. The cells were then permeabilized using 1 % Triton-X in PBS, blocked with 10 % horse serum and stained sequentially with anti-γH2AX(phospho-S139) antibodies, AlexaFluor488-labelled donkey anti-rabbit antibodies (100 μL 1:400 dilution of a 2 mg mL$^{-1}$ stock solution) and DAPI (1 μg mL$^{-1}$ aq. solution), according to standard procedures. The coverslips were mounted onto glass slides and imaged by epifluorescence microscopy as noted above.

## 2.10. Analysis of cell morphology in response to stiffness changes.

The general experimental design is described in the results section below (Section 3.3). MSCs were seeded in individual dishes containing the hydrogel films at a density of 4 x $10^3$ cells cm$^{-2}$, onto hydrogels that had been pre-irradiated with 365 nm light for 30 min. The cells were

cultured in the dark according to section 2.7 for 24 h, irradiated with 490 nm light for 60 min, followed by another 24 h period of culture. As comparators, the cells were cultured for the same period either on gels that were not previously irradiated with 365 nm light, or were not exposed to the 490 nm light. Subsequently, the cells were fixed with formaldehyde and permeabilized as noted above. The fixed samples were blocked with 2 % bovine serum albumin, stained with AlexaFluor488-phalloidin and DAPI according to standard procedures. They were then imaged by epifluorescence microscopy as noted above.

The images were processed in ImageJ (version 2.0.0, National Institutes of Health, USA) and CellProfiler (version 2.1.1, Broad Institute, USA)[47] was used to quantify cell morphometric characteristics. Analysis of variance (ANOVA), Kruskal-Wallis, k-sample-T (KST) and donor-paired t-tests were used as indicated. $p < 0.05$ was used as a threshold for significance. Statistical tests were performed using GraphPad Prism (version 7, GraphPad Software) and Mathematica (version 11.0, Wolfram Research).

In these morphometric analyses, the Kruskal-Wallis test was used to show… while the KST was used to show… [Joe please add a couple of sentences].

## 3. Results and Discussion

### 3.1. Preparation of AZO crosslinker and formulation of AZO-PA hydrogels

In order to prepare the azobenzene-crosslinked polymers, a 4,4'-di(acrylamido)azobenzene ("AZO") crosslinker (Figure 1B) was first synthesized by the acylation of 4,4'-diaminoazobenzene with acryloyl chloride. The structure of AZO allows it to be used as a substitute for the classical *N,N'*-methylenebisacrylamide (BIS) crosslinker in PA hydrogels. In terms of its photophysical properties, AZO was found to photoisomerize (*trans* to *cis*) in solution upon irradiation at 365 nm, reaching a PSS consisting 90.0% *cis* isomer after approximately 30 s (Figures 2A and B). Further

irradiation for up to 1 h resulted in no significant further change. The isomerization could also be reversed (*cis* to *trans*) upon irradiation at 490 nm to a PSS of 86.2 % *trans* isomer after 60 s, with no further change even after 1 h of irradiation (Figures 2C and D).

In order to test the reversibility of isomerization, the compound was subjected to five cycles of irradiation at each wavelength (Figure 2E). Consistent with the above, 90 % *trans* isomer was reached after the first cycle, which represented the PSS. An approximately 2 % loss was observed for every subsequent cycle. Considering the relatively lengthy times of exposure, these results suggested a relatively good photostability for this crosslinker.

Having shown the photoswitchability of the crosslinker in solution, a range of prepolymer formulations containing differing amounts of acrylamide, BIS and AZO in solutions of aqueous buffer were then screened for the formation of clear, stable and homogenous hydrogels upon polymerization (Tables S1–S6 in the Supporting Information). Here, initial efforts aimed at dissolving AZO in a water miscible solvent (i.e. DMSO, DMF, EtOH) that enabled the formation of a homogenous hydrogel. Those formulations that were able to achieve such gels were then tuned to minimize the amount of solvent needed. The inclusion of BIS was also investigated as a means to generate stable hydrogels. Finally, formulations were tested with the aim of maximizing the amount of AZO incorporation. Of those that met these criteria stable, homogenous gels, four formulations (Formulations **56**, **62**, **64** and **83**) that incorporated the highest quantity of AZO crosslinker were taken for further testing.
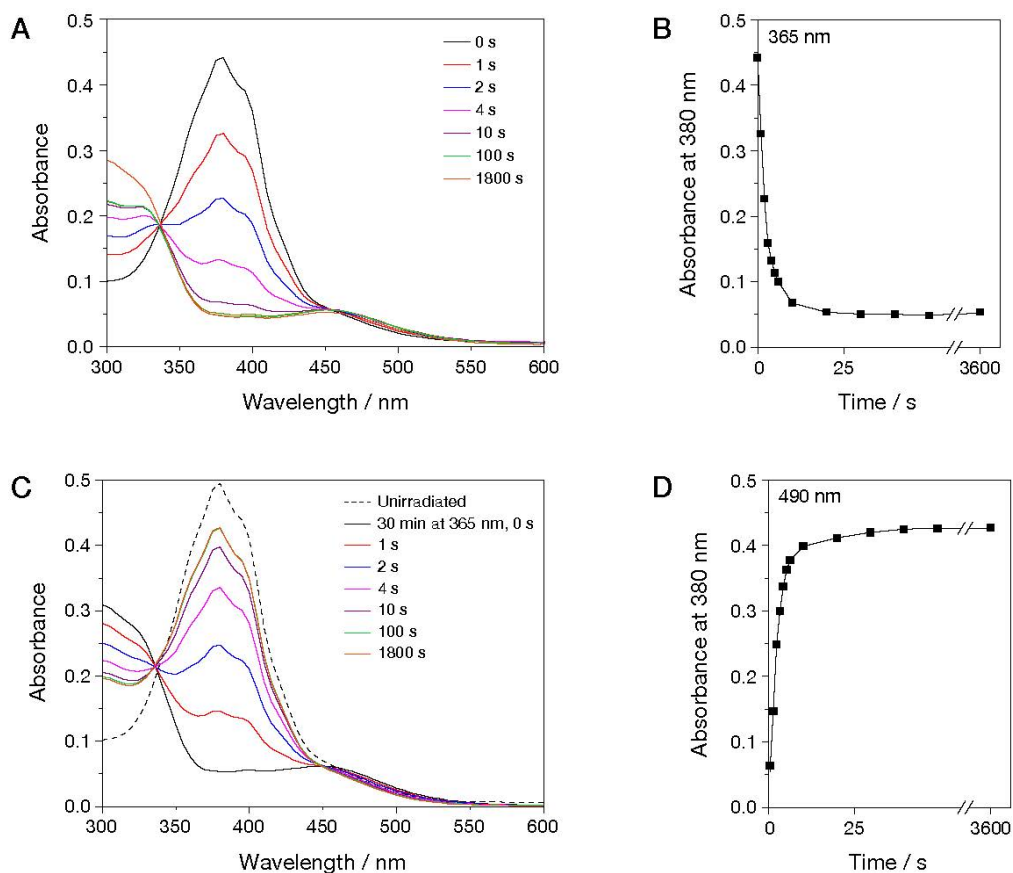
**Figure 2. UV-vis absorbance spectra of AZO.** (A) Sequential absorbance spectra after exposure to 365 nm irradiation for varying amounts of time. (B) Plot of absorbance at the AZO $\lambda_{max}$ (380 nm) against time after 365 nm irradiation. (C) Sequential absorbance spectra after exposure to 365 nm irradiation for 30 min followed by 490 nm for varying amounts of time. (D) Plot of absorbance at the AZO $\lambda_{max}$ (380 nm) against time after 490 nm irradiation, showing the degree of reversibility in photoisomerization. (E) Graph of % *trans*-isomer after each photoswitching cycle for AZO.

*3.2. Mechanical characterization of AZO-PA hydrogels*

The Young's modulus of the four candidate hydrogels were measured by AFM before and after photo-irradiation at 365 nm. As expected, a trend towards increasing stiffness could be observed with increasing amounts of monomer and crosslinker in the hydrogels (Figure 3A). Of

these candidates, formulation **83** was found to give the largest dynamic range with a pre-exposure stiffness of $8.3 \pm 2.0$ kPa that reduced to $2.0 \pm 0.6$ kPa after irradiation at 365 nm, comparable with previously reported materials that use photo-cleavable crosslinkers.[32,33] In terms of proportion, this result represents a 75.9 % reduction in stiffness.

Formulation **83** was thus taken for further mechanical stability studies. The hydrogel was irradiated at 365 nm for 3 h followed by storage in the dark at 37 °C for two weeks to allow for a gradual thermal reversion. The stiffness of the sample was measured at various intervals throughout and it was found that the stiffness of the gel only recovered to $4.5 \pm 0.7$ kPa after two weeks, with little apparent change in stiffness after 6 days (Figure 3B). In order to test whether relatively long UV exposure may have resulted in the degradation of the AZO linkers and the loss of full reversibility, a thermal reversibility experiment was carried out. Here, the hydrogel was irradiated for 3 h, warmed to 60 °C for 16 h, then stored in the dark at ambient temperature (~ 25 °C) for two weeks (Figure 3C). It was observed that the stiffness had increased to $4.3 \pm 0.8$ kPa immediately after the thermal treatment and was fully reversed ($9.0 \pm 3.0$ kPa) at the end of the storage period. These observations indicated that the hydrogel's stiffness was fully reversible, but only extremely slowly. This low rate of background reversibility therefore enables longer term (days to weeks) experiments such that it would make a suitable material for the proposed cell culture applications.
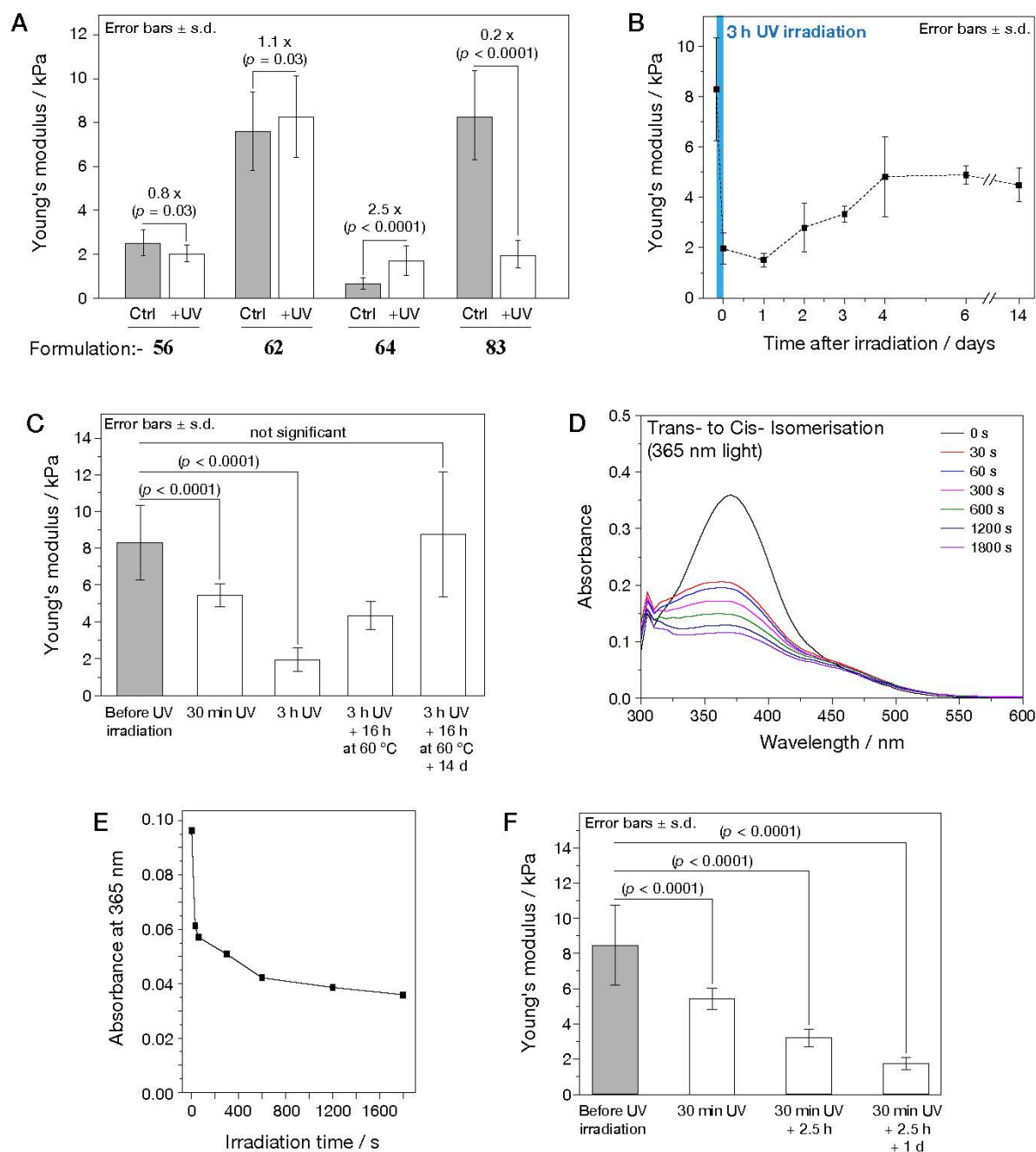
**Figure 3. Mechanical analysis of hydrogels.** (A) Chart of Young's modulus measurements of the hydrogels made from the four lead candidate formulations comparing the differences between before and after 3 h photoirradiation at 365 nm. (B) Graph of Young's modulus against time after 3 h photoirradiation at 365 nm for the hydrogel from formulation **83**. (C) Chart of Young's modulus against time after 3 h photoirradiation at 365 nm for the hydrogel from formulation **83**

and upon prolonged storage. (D) UV-vis spectra of the hydrogel after exposure to light at 365 nm for varying amounts of time and; (E) Graph of UV-vis absorbance at 365 nm against time. (F) Young's modulus of the AZO hydrogel after 30 min irradiation at 365 nm followed by various rest periods. p-Values indicated from Kruskal-Wallis tests.

Notably, the subsequent analysis of the hydrogels by UV-visible spectroscopy showed that the *trans*-azobenzene group had reached the PSS within approximately 30 min of irradiation with 365 nm light (Figures 3D, E). This difference in rapid isomerization of the crosslinker relative to the change in macroscopic stiffness is thought to be due to a requirement for the remodelling of the polymer matrix, which is much slower than the rate of molecular photoisomerization. This delayed change in physical properties is consistent with reports of other hydrogel materials incorporating azobenzene switches.[48]

Since only 30 min of irradiation was sufficient to reach PSS yet approximately 3 h was needed to reach minimum stiffness, a range of shorter irradiation times were investigated followed by a rest period before the stiffness measurements (Figure 3F). It was found that irradiation for 30 min followed incubation of the material in the dark for 2.5 h under ambient conditions resulted in a repeatable stiffness change to 2.5 ± 0.2 kPa. This optimised regime was therefore used for subsequent experiments.

### 3.3. Light induced softening and stiffening of AZO-PA hydrogels

Formulation **83** of the AZO-PA hydrogel was adapted to a platform that would enable the material to be used as a substrate for cell culture. As cells cannot adhere directly to polyacrylamide, the substrate was coated with a layer of fibronectin, providing binding sites for cell attachment.

Previously, methods have been developed to attach a variety of alternative ECM proteins, including collagen-I, collagen-IV and laminin. Alternating the composition of the surface coating offers further opportunity to modulate cell behaviour by activating different integrin receptors at the cell membrane.[9]

In order to enable a study of the interaction between cells and the AZO-PA hydrogels, a two-day experimental programme was designed (Figure 4A). First, the mechanical properties of the culture substrates were measured in the absence of cells. Analysis by AFM showed the fibronectin-coated hydrogels to be significantly softened by exposure to UV light (as described previously), measured 48 h after irradiation (sample "(-) blue" in Figure 4B), compared to a control sample that was kept in the dark (sample "ctrl"). In contrast, exposure of the gels to blue light (60 min at 490 nm) after 24 h caused the stiffness to be significantly recovered at 48 h (sample "(+) blue") $7.6 \pm 0.2$ kPa.
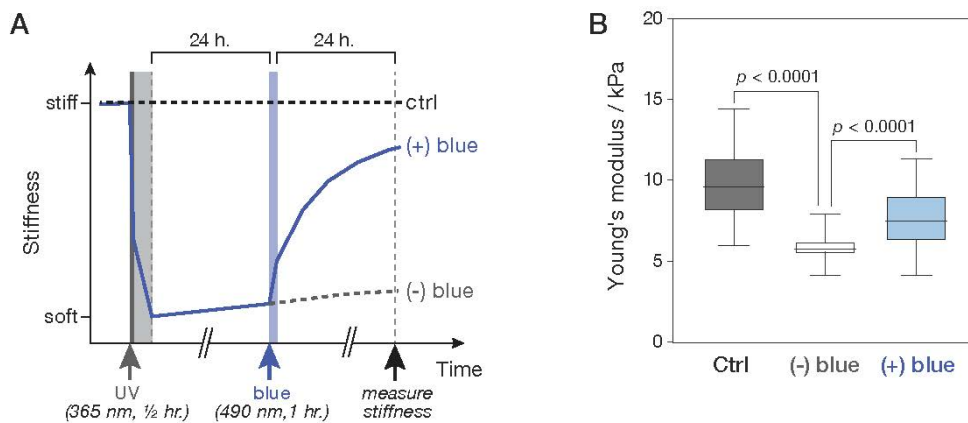


**Figure 4. Hydrogel softening and stiffening by irradiation.** (A) Schematic overview of experiment design showing treatments of photo-responsive hydrogels prior to mechanical characterization. Following preparation, fibronectin-coated gels were softened by exposure to UV (365 nm) irradiation for 30 minutes; 24 h later "(+) blue" gels were exposed to blue (490 nm) light

for 1 hour, while "(-) blue" gels were unirradiated (in the dark). Stiffness measurements were made after a further 24 h, and compared to control gels ("ctrl") that had not been exposed to UV or blue light. (B) Plot of hydrogel stiffnesses obtained by AFM. (-) blue gels were significantly softer than controls, $5.9 \pm 0.1$ kPa vs. $9.7 \pm 0.2$ kPa. Stiffness was significantly increased to $7.6 \pm 0.2$ kPa in (+) blue gels ($\pm$ S.E.M.; $n > 97$ measurements; $p$-values indicated from Kruskal-Wallis tests).

*3.4. Substrates examined by electron microscopy exhibit morphologies typical of hydrogels.*

The light-responsive hydrogels were imaged with scanning electron microscopy (SEM) under the same conditions as the mechanical characterization, i.e. with no exposure to UV irradiation ("ctrl"), with UV irradiation ("(-) blue", softer state), and with UV followed by blue irradiation ("(+) blue", returned to a stiffer state). The surface topology in all cases exhibited a branched network-like structure, with pores in the order of 5 – 20 µm in diameter (Figure 5A-C). This observation was consistent with earlier SEM characterizations of hydrogel morphology, including of polyacrylamide hydrogels with conventional bis-acrylamide crosslinkers,[49] polyvinyl alcohol-based[50] and protein-based hydrogels[51].

Previous reports of characterization of hydrogels by SEM have suggested that the pore structures may form as samples were freeze-dried for imaging [52]. Nonetheless, the AZO-PA hydrogels showed distinct morphological characteristics following the irradiation treatments: the pores appeared to be smaller in the "(-) blue" sample (Figure 5B), but were returned to a larger size following exposure to blue light, although the structure appeared less ordered (Figure 5C). These results were consistent with previous reports where an inverse relationship was found between the size of pores observed by SEM and the stiffnesses of hydrogels formed by varying the relative concentrations of polyacrylamide and conventional crosslinkers.[49] This observation

further supports the view that the mechanisms by which hydrogel stiffness is altered by photoirradiation is not due only to the switching of the AZO conformation, but that switching subsequently results in the reorganization of the overall polymer matrix.
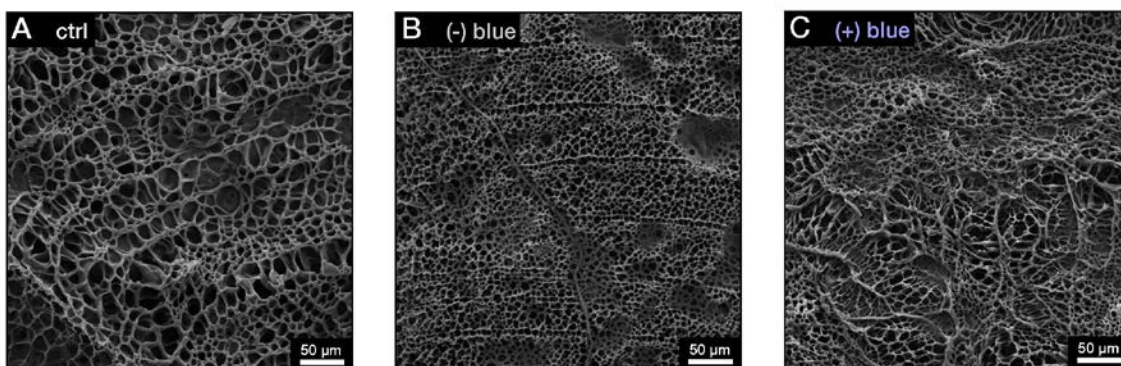


**Figure 5. Scanning electron micrographs of photo-responsive hydrogels before and after irradiation.** The images were recorded following the treatments indicated in Figure 4A at the point of "stiffness measurement". (A) Control ("ctrl") sample: AZO hydrogels not subjected to irradiation. (B) "(-) blue" sample: hydrogel treated with UV (365 nm) irradiation. (C) "(+) blue" sample: hydrogel treated with UV (365 nm) and subsequent blue light (490 nm) irradiation.

These materials were also subsequently subjected to microscopy under environmental SEM (ESEM), which enabled the imaging of the hydrated gels under near ambient conditions (Figure 6 and Figure S2 in SI). In all cases, these images showed a uniform surface with apparent "pore" features in the nanometre size regime. However, the quality of the images at this magnification was not sufficiently well resolved to perform fully quantitative measurements, however several manual measurements suggest pore widths of approximately 30–50 nm; far below the size of biological cells.

**Figure 6. Environmental scanning electron micrographs of photo-responsive hydrogels before and after irradiation.** The images were recorded following the treatments indicated in Figure 4A at the point of "stiffness measurement". (A) Control ("ctrl") sample: AZO hydrogels not subjected to irradiation. (B) "(-) blue" sample: hydrogel treated with UV (365 nm) irradiation. (C) "(+) blue" sample: hydrogel treated with UV (365 nm) and subsequent blue light (490 nm) irradiation.

*3.5. The effect of irradiation conditions on MSC viability*

Once the dosage of light that was necessary for isomerization had been established, the next phase of investigation to determine the extent to which irradiation would in itself affect cell behaviour, irrespective of substrate mechanics. Cells *in vitro* culture were therefore subjected to matched irradiation regimes and assayed for viability and damage to DNA.

Primary human mesenchymal stem cells (MSCs) cultured under standard conditions were subjected to irradiation and viability was assessed by established live/dead staining (Figure S3A in SI). Exposure to light emitted from a blue LED for up to 1 h did not significantly alter cell viability, compared to control cells without irradiation. In contrast, exposure to just 10 min of UV light was sufficient to reduce cell viability to $18 \pm 8$ % of the control (Figure S3B in SI).

DNA double-strand breaks (DSBs) are particularly deleterious to cell viability, and can occur where DNA replication forks are arrested following UV irradiation.[53] In response to DNA damage, a cascade of kinase signalling pathways result in the phosphorylation of the histone variant H2AX. This phosphorylated histone ("γH2AX") accumulates at DSBs and the immuno-staining of γH2AX foci can be used as a basis for quantifying the extent of DNA damage.[54] Following irradiation, the number of focal points of DNA damage counted in each nucleus by staining with an antibody against serine-139 phosphorylated γH2AX (Figure S4A in SI).

Irradiation with blue light for up to 60 min did not increase the number of γH2AX foci above a baseline set by a control sample of cells cultured in the dark (Figure S4B in SI). However, exposure to UV light for just 10 min was sufficient to cause so much γH2AX staining in the nuclei that individual foci could not be distinguished.

In summary, exposure to blue light had no detrimental effect on MSC viability, but exposure to UV irradiation for 10 min caused sufficient DNA damage to greatly limit cell viability. Subsequent cell culture experiments were thus designed such that UV irradiation was performed prior to cell seeding onto the gels.

*3.6. Substrates enable light-induced modulation of MSC morphology*

The MSC response to culture on stiffness-tuneable substrates was assessed according to the following scheme (Figure 7A). Fibronectin-coated AZO-PA hydrogels were first softened by exposure to UV light (30 min at 365 nm), and only subsequently were primary human MSCs seeded onto the softened hydrogels, thus avoiding any cell exposure to UV irradiation. As a control, MSCs were also seeded onto a hydrogel that had not been subjected to irradiation ("ctrl"). After 24 h a set of cells on UV-softened substrates were subjected to blue-light irradiation ("(+) blue"), while a second set of cells on UV-softened substrates were maintained in the dark ("(-) blue"). All cell samples were cultured for a total of 48 h before being fixed for imaging. This work was undertaken with primary human MSCs because of their potential for application in medical and tissue engineering applications,[13] but primary cells are subject to donor-to-donor variation. Thus, this study employed MSCs sourced from multiple donors, therefore ensuring reproducibility and robustness of both the hydrogel platform and the biological response. After fixing, the cell nuclei were stained with DAPI and the actin cytoskeleton with phalloidin, thus allowing cell morphology to be readily assessed.

Cells adhered, spread and flattened on the hydrogels, exhibiting a morphology typical of MSCs and adherent cells cultured on two-dimensional substrates, indicating successful cellular attachment to the fibronectin coating. Cell adherence was maintained over the 48 h course of the experiment and an assessment of cell viability by established live/dead staining (Figure 7B), which showed that. Furthermore, it was observed that the cells did not show the rounded morphologies typical of apoptosis, suggesting that the hydrogel chemistry was not intrinsically toxic (Figure 7C). Additionally, cells were imaged in a single focal plane, indicating that the cells were adhering to the substrate surface and were not penetrating into the pores identified in SEM images, which typically had sub-cellular dimensions. Finally, for practical purposes, the cells could be imaged effectively on the hydrogels without interference from high background autofluorescence.
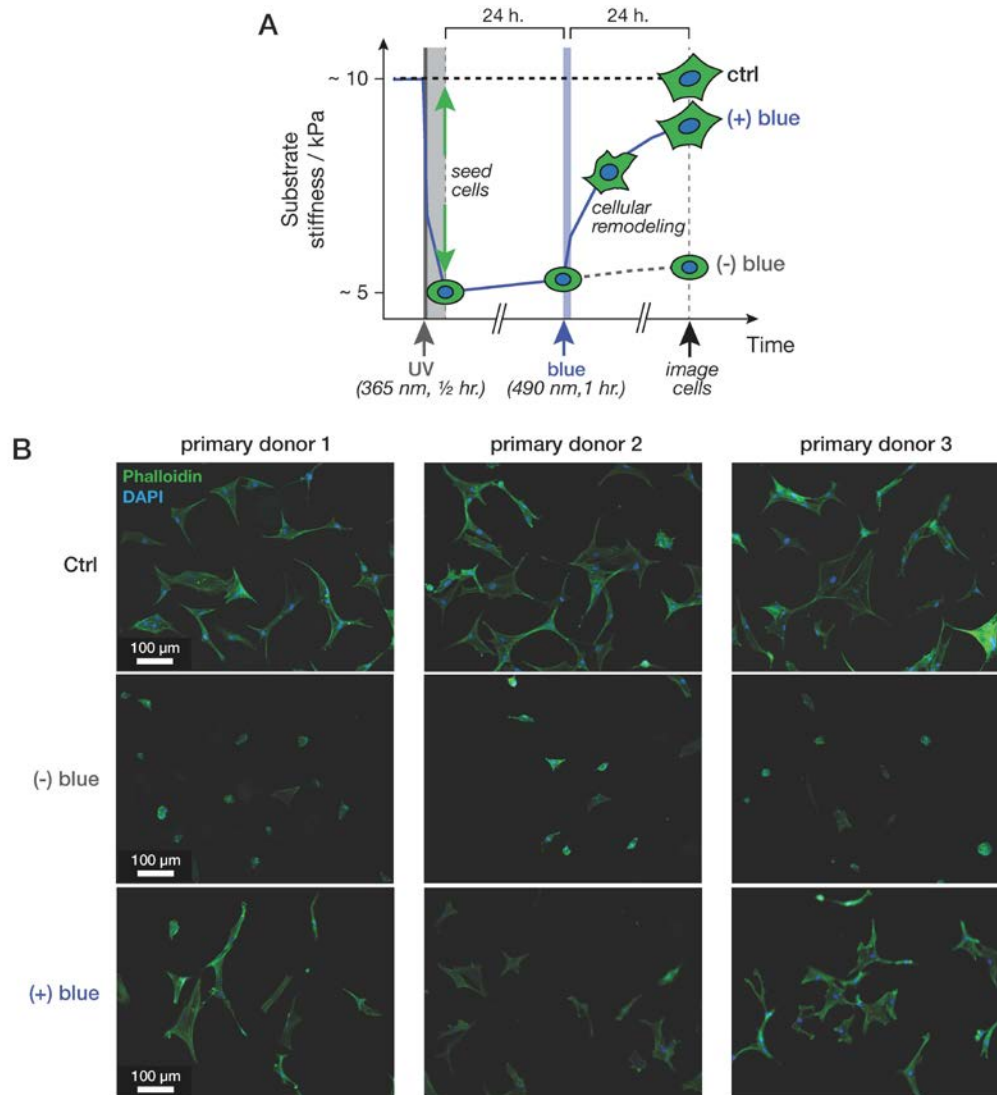
**Figure 7. Mesenchymal stem cell (MSC) culture on photoresponsive hydrogels.** (A) Schematic overview of cell culture experiments on photo-responsive hydrogels. Fibronectin-coated gels were softened by exposure to UV (365 nm) irradiation for 30 minutes. Primary human MSCs were then seeded. After 24 h, "(+) blue" gels were exposed to blue (490 nm) light for 1 hour, while "(-) blue" gels were kept in darkness. Cells were fixed for imaging after a further 24 h, and compared to cells cultured on control gels ("ctrl") that had not been exposed to UV or blue light. (B) Plot of (C) High-resolution images of MSCs from multiple primary human donors on photo-responsive

hydrogels. Cells in all conditions were seeded and fixed at the same times and stained with DAPI (blue) and phalloidin (green).

Cell morphology is robustly coupled to substrate stiffness, with many types of adherent cell spreading to a greater degree on stiffer substrates.[31,55,56] Features such as the alignment of actin stress fibres are also influenced by substrate stiffness.[57] Furthermore, characterizations of morphological features, such as spread cell area and cytoskeletal features, have been shown to be highly predictive of cell fate.[58] Imaging of the MSCs on AZO-PA substrates after 48 h showed "ctrl" cells to be well spread, "(-) blue" cells to be smaller, and "(+) blue" cells to have recovered spreading (Figure 7C).

To gain further insight into cell morphometrics, images of MSCs on the AZO-PA gels were subject to quantitative image analysis. It was found that the spread cell area was significantly lower in "(-) blue" samples than "ctrl" in each of five biological replicates, with the mean spread area reduced from $1090 \pm 60$ to $500 \pm 40\,\mu m^2$ (donor-paired t-test $p = 0.003$; Figures 8A-C). This spread cell area was recovered in "(+) blue" samples in each of the five biological replicates. In two of the donors, the areas of the blue-irradiated cells were not significantly different from the "ctrl" sample (Figure 8B). The mean recovered spread area in the "(+) blue" samples was $940 \pm 50\,\mu m^2$ (donor-paired t-test $p = 0.002$ for difference from "(-) blue" samples; Figures 8C). It was also found that the cell spread area can be used as a readout of stiffness, as "sensed" by the cells, by calibrating against a standard of bis-acrylamide crosslinked polyacrylamide gels prepared in accordance with previous literature[9] (coated with fibronectin). This method suggested that the "ctrl" gels had a stiffness of ~3 kPa, were softened to ~1.5 kPa in the "(-) blue" treatment, but were recovered to ~2.5 kPa in "(+) blue" samples (Figure 8D). These values are slightly lower than

those measured by AFM (Figure 4B), but the trend was maintained and the magnitudes of fold-changes were similar.

Since the nucleus is physically connected to the cytoskeleton by the linker of nucleoskeleton and cytoskeleton (LINC) complex, changes in cellular morphology often propagate to the nucleus, a mechanism likely to influence the transduction of mechanical signalling.[59] Consistent with this hypothesis, the mean projected nuclear area was slightly reduced relative to "ctrl" in "(-) blue" samples, but recovered in "(+) blue" samples. However, these trends were not statistically significant (Figure 8E). The cell aspect ratio (defined by the ratio of lengths of long to small sides of a rectangle bounding the cell) was found to be significantly lower in the "(-) blue" sample relative to "ctrl" ($p = 0.03$), and significantly recovered in "(+) blue" ($p = 0.05$; Figure 8F). Correspondingly, cell circularity (proportional to the area divided by the square of the perimeter) was significantly increased in the "(-) blue" sample relative to "ctrl" ($p = 0.02$), and reduced again in "(+) blue" ($p = 0.05$; Figure 8G). Each of these morphological characterizations is consistent with the response of MSCs to changes in substrate stiffness reported in earlier literature.
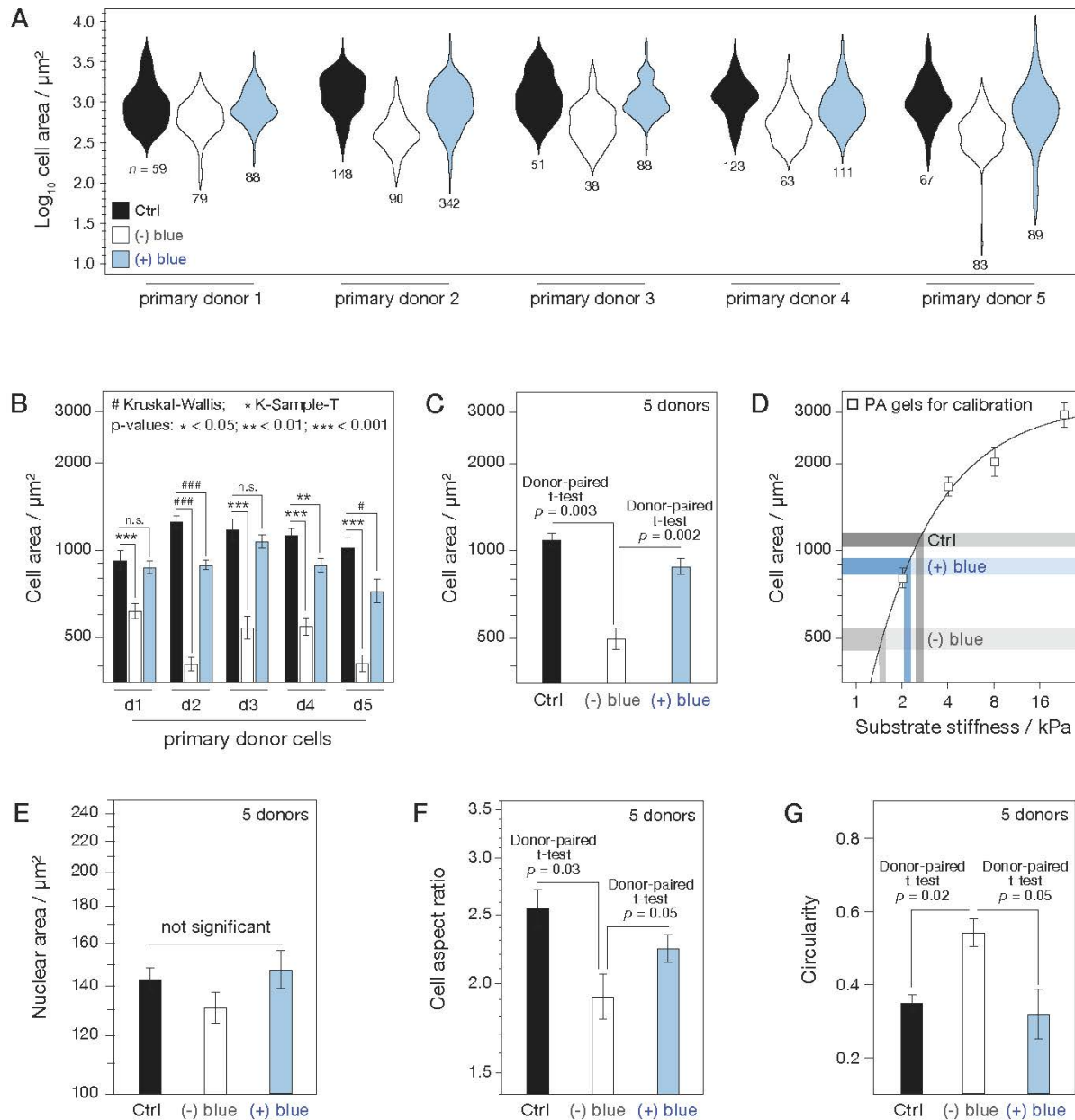
**Figure 8. Quantitative morphometric analysis of mesenchymal stem cells (MSCs) on photoresponsive hydrogels.** (A) Distribution plots of MSC spread areas, following treatments shown in Figure 7A (*n* indicates number of cells analysed). (B) Cell spread areas were consistently suppressed in "(-) blue" samples, indicative of a softer substrate [60], but recovered in "(+) blue" samples. (C) Donor-paired t-tests confirmed that MSC spread area was significantly reduced under "(-) blue" conditions, $500 \pm 40$ vs. $1090 \pm 60$ $\mu m^2$ ($\pm$ S.E.M.; $p = 0.003$), and that spreading was

significantly recovered by blue light exposure, to $940 \pm 50 \ \mu m^2$ ($\pm$ S.E.M.; $p = 0.002$). (D) Cell spread areas on photo-responsive gels were compared to those on polyacrylamide gels prepared according to established formulations [9] and used as a "cellular calibration" of stiffness. (E) Nuclear spread areas correlated with trends seen in cell spread areas [16], although changes were not significant. (F) Cell aspect were significantly reduced in "(-) blue" samples and recovered in "(+) blue" samples. (G) Cell circularity was significantly increased in "(-) blue" samples and recovered in "(+) blue" samples (statistical tests as indicated).

## 4. Conclusions

MSCs have well characterized mechano-responses, where the phenotype can be influenced by substrate stiffness and topology at micron and nanometer scales. The AZO-PA hydrogel was able to modulate MSC behavior through alteration of substrate mechanics in response to stimulation that was otherwise "invisible" to the cells. In comparison to an earlier azobenzene-incorporating hydrogel,[40] this material demonstrates a superior dynamic range (75.9 % reduction *vs.* ~ 2%) and a longer maintenance of the softer "on" state (2 weeks *vs.* ~ 10 h). It could therefore be used as a platform to study mechano-signalling in cells responding to dynamic and potentially spatially defined changes, over biologically relevant stiffnesses and timescales.

Further materials development in this area will benefit from the incorporation of advanced designs of azobenzene crosslinkers with tuneable photoabsorption[61,62] that circumvent the need for detrimental UV light. The dynamic range (i.e. the difference in stiffness achieved upon switching) could also be improved by reengineering of the crosslinker to increase its solubility in aqueous media, as it would enable the incorporation of larger amounts into the polymer.

From a biological perspective, future work will apply this technology to better understand mechano-transduction signalling pathways, and also biological processes with implicit changes to tissue mechanics, such as development,[26] ageing[63] and fibrosis[24].

**Supporting Information**

- Tables of prepolymer formulations tested.

- Schematic diagram of the substrate preparation for cell culture.

- Low magnification ESEM micrographs of hydrogels.

- Supplementary results related to studies of cell viability and DNA damage following photoirradiation.

**Acknowledgments**

**References**

1.      Winer, J. P.; Janmey, P. A.; McCormick, M. E.; Funaki, M., *Tissue Eng.* **2009,** *15*, 147-154.

2.      Georges, P. C.; Miller, W. J.; Meaney, D. F.; Sawyer, E. S.; Janmey, P. A., *Biophys. J.* **2006,** *90*, 3012-3018.

3.      Guilak, F.; Alexopoulos, L. G.; Haider, M. A.; Ting-Beall, H. P.; Setton, L. A., *Ann. Biomed. Eng.* **2005,** *33*, 1312-1318.

4.      Engler, A. J.; Sen, S.; Sweeney, H. L.; Discher, D. E., *Cell* **2006,** *126*, 677-689.

5.      Pelham, R. J.; Wang, Y. L., *Proc. Natl. Acad. Sci.* **1997,** *94*, 13661-13665.

6.      Discher, D. E.; Janmey, P.; Wang, Y. L., *Science* **2005,** *310*, 1139-1143.

7.      Hennink, W. E.; van Nostrum, C. F., *Adv. Drug Deliv. Rev.* **2012,** *64*, 223-236.

8.      Baroli, B., *J. Pharm. Sci.* **2007,** *96*, 2197-2223.

9.      Tse, J. R.; Engler, A. J., *Curr. Protoc. Cell Biol.* **2010,** *47*, 16.10-16.16.

10.     Lo, C. M.; Wang, H. B.; Dembo, M.; Wang, Y. L., *Biophys. J.* **2000,** *79*, 144-152.

11.     Klein, E. A.; Yin, L.; Kothapalli, D.; Castagnino, P.; Byfield, F. J.; Xu, T.; Levental, I.; Hawthorne, E.; Janmey, P. A.; Assoian, R. K., *Curr. Biol.* **2009,** *19*, 1511-1518.

12.     Wang, H. B.; Dembo, M.; Wang, Y. L., *Am. J. Physiol. Cell Physiol.* **2000,** *279*, C1345-C1350.

13.     Richardson, S. M.; Hoyland, J. A.; Mobasheri, R.; Csaki, C.; Shakibaei, M.; Mobasheri, A., *J. Cell. Physiol.* **2010,** *222*, 23-32.

14.     Tolar, J.; Le Blanc, K.; Keating, A.; Blazar, B. R., *Stem Cells* **2010,** *28*, 1446-1455.

15.     Steinert, A. F.; Rackwitz, L.; Gilbert, F.; Noth, U.; Tuan, R. S., *Stem Cells Transl. Med.* **2012,** *1*, 237-247.

16.     Swift, J.; Ivanovska, I. L.; Buxboim, A.; Harada, T.; Dingal, P. C. D. P.; Pinter, J.; Pajerowski, J. D.; Spinler, K. R.; Shin, J.-W.; Tewari, M.; Rehfeldt, F.; Speicher, D. W.; Discher, D. E., *Science* **2013,** *341*, 1240104.

17.     Pittenger, M. F.; Mackay, A. M.; Beck, S. C.; Jaiswal, R. K.; Douglas, R.; Mosca, J. D.; Moorman, M. A.; Simonetti, D. W.; Craig, S.; Marshak, D. R., *Science* **1999,** *284*, 143-147.

18.     Matthews, B. D.; Thodeti, C. K.; Tytell, J. D.; Mammoto, A.; Overby, D. R.; Ingber, D. E., *Integr. Biol.* **2010,** *2*, 435-442.

19.     Bershadsky, A. D.; Balaban, N. Q.; Geiger, B., *Annu. Rev. Cell Dev. Biol.* **2003,** *19*, 677-695.

20.     Makhija, E.; Jokhun, D. S.; Shivashankar, G. V., *Proc. Natl. Acad. Sci.* **2016,** *113*, E32-E40.

21.     Dupont, S.; Morsut, L.; Aragona, M.; Enzo, E.; Giulitti, S.; Cordenonsi, M.; Zanconato, F.; Le Digabel, J.; Forcato, M.; Bicciato, S.; Elvassore, N.; Piccolo, S., *Nature* **2011,** *474*, 179-183.

22.     Connelly, J. T.; Gautrot, J. E.; Trappmann, B.; Tan, D. W. M.; Donati, G.; Huck, W. T. S.; Watt, F. M., *Nat. Cell Biol.* **2010,** *12*, 711-718.

23.     Dingal, P. C. D. P.; Bradshaw, A. M.; Cho, S.; Raab, M.; Buxboim, A.; Swift, J.; Discher, D. E., *Nat. Mater.* **2015,** *14*, 951-960.

24.     Li, C. X.; Talele, N. P.; Boo, S.; Koehler, A.; Knee-Walden, E.; Balestrini, J. L.; Speight, P.; Kapus, A.; Hinz, B., *Nat. Mater.* **2017,** *16*, 379-389.

25.     Young, J. L.; Engler, A. J., *Biomaterials* **2011,** *32*, 1002-1009.

26.     Majkut, S.; Idema, T.; Swift, J.; Krieger, C.; Liu, A.; Discher, D. E., *Curr. Biol.* **2013,** *23*, 2434-2439.

27.     Berry, M. F.; Engler, A. J.; Woo, Y. J.; Pirolli, T. J.; Bish, L. T.; Jayasankar, V.; Morine, K. J.; Gardner, T. J.; Discher, D. E.; Sweeney, H. L., *Am. J. Physiol. Heart Circ. Physiol.* **2006,** *290*, H2196-H2203.

28. Humphrey, J. D.; Dufresne, E. R.; Schwartz, M. A., *Nat. Rev. Mol. Cell Biol.* **2014,** *15*, 802-812.

29. Sherratt, M. J., *Age* **2009,** *31*, 305-325.

30. Gillette, B. M.; Jensen, J. A.; Wang, M. X.; Tchao, J.; Sia, S. K., *Adv. Mater.* **2010,** *22*, 686-691.

31. Yoshikawa, H. Y.; Rossetti, F. F.; Kaufmann, S.; Kaindl, T.; Madsen, J.; Engel, U.; Lewis, A. L.; Armes, S. P.; Tanaka, M., *J. Am. Chem. Soc.* **2011,** *133*, 1367-1374.

32. Yang, C.; Tibbitt, M. W.; Basta, L.; Anseth, K. S., *Nat. Mater.* **2014,** *13*, 645-652.

33. Frey, M. T.; Wang, Y. L., *Soft Matter* **2009,** *5*, 1918-1924.

34. Guvendiren, M.; Burdick, J. A., *Nat. Commun.* **2012,** *3*, 792.

35. Rosales, A. M.; Vega, S. L.; DelRio, F. W.; Burdick, J. A.; Anseth, K. S., *Angew. Chem. Int. Ed.* **2017,** *56*, 12132-12136.

36. Beharry, A. A.; Woolley, G. A., *Chem. Soc. Rev.* **2011,** *40*, 4422-4437.

37. Brieke, C.; Rohrbach, F.; Gottschalk, A.; Mayer, G.; Heckel, A., *Angew. Chem. Int. Ed.* **2012,** *51*, 8446-8476.

38. Liu, J. W.; Nie, J.; Zhao, Y. F.; He, Y., *J. Photochem. Photobiol. A* **2010,** *211*, 20-25.

39. Zhang, Q. M.; Li, X.; Islam, M. R.; Wei, M. L.; Serpe, M. J., *J. Mater. Chem. C* **2014,** *2*, 6961-6965.

40. Rosales, A. M.; Mabry, K. M.; Nehls, E. M.; Anseth, K. S., *Biomacromolecules* **2015,** *16*, 798-806.

41. Hatchard, C. G.; Parker, C. A., *Proc. Roy. Soc. A* **1956,** *235*, 518-536.

42. Thompson, M. P.; Agger, J.; Wong, L. S., *J. Chem. Educ.* **2015,** *92*, 1716-1720.

43.     Weston, C. E.; Richardson, R. D.; Haycock, P. R.; White, A. J. P.; Fuchter, M. J., *J. Am. Chem. Soc.* **2014,** *136*, 11878-11881.

44.     Weston, C. E.; Richardson, R. D.; Haycock, P. R.; White, A. J. P.; Fuchter, M. J., *J. Am. Chem. Soc.* **2016,** *138*, 10716-10716.

45.     Rosenbluth, M. J.; Lam, W. A.; Fletcher, D. A., *Biophys. J.* **2006,** *90*, 2994-3003.

46.     Strassburg, S.; Richardson, S. M.; Freemont, A. J.; Hoyland, J. A., *Regen. Med.* **2010,** *5*, 701-711.

47.     Kamentsky, L.; Jones, T. R.; Fraser, A.; Bray, M. A.; Logan, D. J.; Madden, K. L.; Ljosa, V.; Rueden, C.; Eliceiri, K. W.; Carpenter, A. E., *Bioinformatics* **2011,** *27*, 1179-1180.

48.     Li, Y. B.; He, Y. N.; Tong, X. L.; Wang, X. G., *J. Am. Chem. Soc.* **2005,** *127*, 2402-2403.

49.     Trappmann, B.; Gautrot, J. E.; Connelly, J. T.; Strange, D. G. T.; Li, Y.; Oyen, M. L.; Cohen Stuart, M. A.; Boehm, H.; Li, B.; Vogel, V.; Spatz, J. P.; Watt, F. M.; Huck, W. T. S., *Nat. Mater.* **2012,** *11*, 642-649.

50.     Zhang, N. Y.; Shen, Y. G.; Li, X. Q.; Cai, S. J.; Liu, M. Z., *Biomed. Mater.* **2012,** *7*, 035014-035025.

51.     Navarra, G.; Peres, C.; Contardi, M.; Picone, P.; Biagio, P. L. S.; Di Carlo, M.; Giacomazza, D.; Militello, V., *Arch. Biochem. Biophys.* **2016,** *606*, 134-142.

52.     Kato, N.; Sakai, Y.; Shibata, S., *Macromolecules* **2003,** *36*, 961-963.

53.     de Feraudy, S.; Revet, I.; Bezrookove, V.; Feeney, L.; Cleaver, J. E., *Proc. Natl. Acad. Sci.* **2010,** *107*, 6870-6875.

54.     Celeste, A.; Fernandez-Capetillo, O.; Kruhlak, M. J.; Pilch, D. R.; Staudt, D. W.; Lee, A.; Bonner, R. F.; Bonner, W. M.; Nussenzweig, A., *Nat. Cell Biol.* **2003,** *5*, 675-679.

55.     Engler, A. J.; Carag-Krieger, C.; Johnson, C. P.; Raab, M.; Tang, H. Y.; Speicher, D. W.; Sanger, J. W.; Sanger, J. M.; Discher, D. E., *J. Cell Sci.* **2008,** *121*, 3794-3802.

56.     Ghibaudo, M.; Saez, A.; Trichet, L.; Xayaphoummine, A.; Browaeys, J.; Silberzan, P.; Buguin, A.; Ladoux, B., *Soft Matter* **2008,** *4*, 1836-1843.

57.     Zemel, A.; Rehfeldt, F.; Brown, A. E. X.; Discher, D. E.; Safran, S. A., *Nat. Phys.* **2010,** *6*, 468-473.

58.     Treiser, M. D.; Yang, E. H.; Gordonov, S.; Cohen, D. M.; Androulakis, I. P.; Kohn, J.; Chen, C. S.; Moghe, P. V., *Proc. Natl. Acad. Sci.* **2010,** *107*, 610-615.

59.     Swift, J.; Discher, D. E., *J. Cell Sci.* **2014,** *127*, 3005-3015.

60.     Engler, A.; Bacakova, L.; Newman, C.; Hategan, A.; Griffin, M.; Discher, D., *Biophys. J.* **2004,** *86*, 617-628.

61.     Calbo, J.; Weston, C. E.; White, A. J. P.; Rzepa, H. S.; Contreras-Garcia, J.; Fuchter, M. J., *J. Am. Chem. Soc.* **2017,** *139*, 1261-1274.

62.     Dong, M.; Babalhavaeji, A.; Collins, C.; Jarrah, K.; Sadovski, O.; Dai, Q.; Woolley, G. A., *J. Am. Chem. Soc.* **2017,** *139*, 13483-13486.

63.     Phillip, J. M.; Aifuwa, I.; Walston, J.; Wirtz, D., *Annu. Rev. Biomed. Eng.* **2015,** *17*, 113-141.

**Graphical Abstract**